ISSN 1062-7391, Journal of Mining Science, 2020, Vol. 56, No. 5, pp. 848–856. © Pleiades Publishing, Ltd., 2020.
Published in Fiziko-Tekhnicheskie Problemy Razrabotki Poleznykh Iskopaemykh, 2020, No. 5, pp. 185–193.

MINERAL DRESSING

The Effects of Ball Size on the Determination of Breakage Parameters of Nepheline Syenite

S. Haner

Department of Industrial Product Design, Afyon Kocatepe University, Afyonkarahisar, Turkey
e-mail: shaner@aku.edu.tr

Received December 16, 2019
Revised August 16, 2020
Accepted September 11, 2020

Abstract—In this study, the changes in the specific rate of breakage and breakage distribution function of the nepheline syenite sample were investigated by using alloy steel ball in five different sizes. Specific rate of breakage and breakage distribution function values were obtained from the particle size distributions acquired after the grinding periods. As a result of grinding tests, an increase in rate of breakage is observed due to the increase in ball diameter.

Keywords: Nepheline syenite, breakage function, specific rate of breakage, fine comminution.

DOI: 10.1134/S1062739120057191

INTRODUCTION

For hundreds of years, feldspathic materials have played a role as melters in the ceramic and glass industry. It is known that the production of feldspar is performed in more than fifty countries worldwide. Turkey has a special place in this competitive environment. Turkey, which has very high quality feldspar deposits, also owns about 14% of the world's feldspar reserves. Granitic rock, nepheline syenite, altered granite, granite sand and pegmatite are produced as commercial feldspar source. Among these sources of feldspar, the properties and economic value of nepheline syenite should be considered separately. Nepheline syenite is a light colored, coarse crystalline, siliciously poor, feldspathic, plutonic magmatic rock. This rock contains mainly nepheline, orthoclase, microcline and albite. Compared to other feldspars, its Na and K ratio is quite high. Nepheline syenite is included in the composition of industrial materials as a source of alumina (>23%) and alkali. There is no free quartz due to low silica (<60%). Economic bearings formations are located in Russia, Canada, Norway, Brazil, United States, China and Turkey [1, 2].

The world nepheline syenite production began in the 1900s. In Turkey, nepheline syenite processing was begun in 2008 by a private company located in Akpınar district Buzlukdağı local which is centralized in Kırşehir. The visible reserve area of the nepheline syenite in this filed has a length of 2250 m, a width of 1850 m and a depth of 450 m [1]. In the enrichment plant located here, crushing, grinding, wet magnetic separation (0.11 $kgs^{-2}A^{-1}$) and drying processes are applied for nepheline syenite. The dried raw material is subjected to dry magnetic separation at a force of 1.2 $kgs^{-2}A^{-1}$ and nepheline syenite is marketed. The aim of magnetic separation results in the increase in K_20:Na_2O ratio, the removal of iron-bearing and other harmful impurities [3]. This enrichment product of nepheline syenite is mainly used in the ceramic industry.

The nepheline syenite obtained by the ceramic plants in a particle size of –0.5 mm is first milled. Ball mills are often used for grinding here. Raw materials such as quartz, feldspar and nepheline syenite, which form the ball mill phase, are milled to a particle size of –0.06 mm. As the particle size

decreases, structural defects of the particles decrease and attrition occurs in the predominant fracture mechanism. In addition, most of the energy spent on grinding is converted into heat energy. Therefore, the economic efficiency of grinding mills with ball mills below 0.1 mm particle size is less. When these limits are exceeded, the specific energies of ball mills increase exponentially [4].

In the studies performed for the cost of traditional ceramic products such as tile, tableware, sanitary ware, brick and heavy clay, the primary consideration should be cooking temperature and duration [5]. However, other than this general idea, the biggest share in the cost of a ceramic product is the raw material cost (RC) and the raw material preparation cost (RPC). RC includes the mining company's expenses (open pit cost, crushing, screening, grinding, enrichment, personnel, accommodation, etc.) and profit. RPC includes ceramic production expenditures (crushing, screening, transport and grinding) expect product-baking. For example, in wall tile production, RC and RPC account for approximately 58% of the total production cost and natural gas consumption accounts for 42% [6]. In order to reduce the costs of RC and RPC, it is necessary to obtain optimum values in the size reduction process of raw materials. According to Plaksin, Uteush, and Uteush (1965, 4), "[t]he most expensive process in enrichment plants is grinding the ore (50–60% of the total cost). In many respects, this process determines the results to be obtained from subsequent processes (flotation, magnetic separation, etc.)."[7]. For this, appropriate equipment should be selected, operating variables should be well defined and the effects of changes in these variables should be determined accurately.

The grinding process, which is one of the important components of RC and RPC, constitutes the final stage of the size reduction processes. Grinding can generally be classified into coarse, intermediate, and fine grinding processes. This classification difference is due to the grinding equipment used, the product size distribution and the comminution mechanisms. In coarse grinding typically corresponds to an AG/SAG mill ($F_{80} = 0.50$–10 mm), intermediate grinding to a ball mill ($F_{80} = 0.040$–0.40 mm) or tower mill ($F_{80} = 0.040$–0.40 mm), and fine grinding to a stirred mill ($F_{80} < 0.030$ mm) [8].

An important variable affecting the capacity and efficiency of mills is the size of the grinding material. There are some approaches in the literature regarding the selection of optimum media sizing in the intermediate grinding process with a ball mill [9–12]. Among these approaches, the formula stated below, which is the most widely used in the industry, was presented by Bond (1958):

$$B = \left(\frac{F_{80}}{K}\right)^{0.5} \left(\frac{SW_i}{C_s D^{0.5}}\right)^{1/3},$$

where B is the recommended make-up ball size, inches; F_{80} is the circuit feed 80 percent passing size, microns; K is constant (for wet overflow mills $K = 350$); W_i is the Bond Test Work Index, kWh/t; S is the ore specific gravity; C_s is the mill speed in percent of critical, %; D is the mill inside (liners, working) diameter, feet.

However, the Bond method is a long process and does not give an exact idea about the particle size fractions. Therefore, some mathematical models have been developed. In the kinetic model created by Lynch and developed by Austin, there are mathematical expressions defining the rate of breakage and breakage distribution function of a raw material [13]. Laboratory-wide values obtained by kinetic model-based grinding studies are suitable for simulation in an industrial environment [14].

In this study, using the kinetic model developed by Austin, Klimpel, and Luckie (1984), the breakage parameters of nepheline syenite in Kırşehir, Akpınar (Turkey) were determined. In order to observe the change of specific rate of breakage and breakage distribution function alloy steel ball was used in five different sizes.

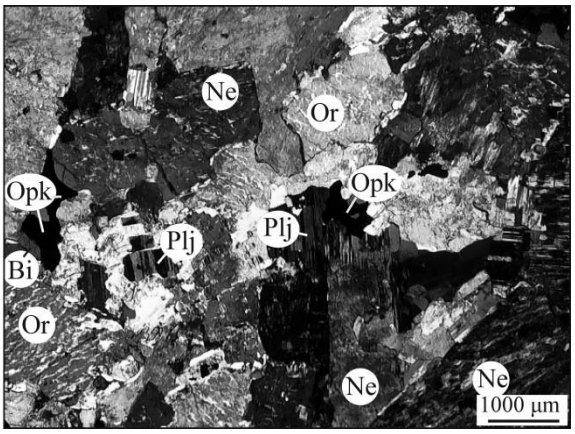

Fig. 1. Thin section images of nepheline syenite: Ne—nepheline, Or—orthoclase, Plj—plagioclase, Bi—biotite, Opq—opaque mineral.

1. MATERIALS AND METHODS

The nepheline syenite used in the grinding studies based on the kinetic model was obtained from a private mining company located in Akpınar district of Kırşehir province. Chemical analysis values of nepheline syenite are:

SiO_2	65.22
Al_2O_3	19.47
K_2O	8.74
Na_2O	5.00
CaO	1.04
MgO	0.03
Fe_2O_3	0.29
TiO_2	0.07
MnO	0.01
Loss in ignition	0.13

Thin section investigations were made from different aspects of nepheline syenite rock. Representative images are shown in Fig. 1. As a result of these investigations, it is identified that the rock contains 30–35% nephelin, 25–30% orthoclase, 10–15% microline, 8–10% plagioclase (albite-oligoclas), 4–5% biotite, 3–7% clino pyroxene (aegirine-augite), 2–5% opaque minerals. It is generally seen that an equigranular/holocrystalline texture is dominant in the rock.

The nepheline has a subhedral, euhedral, angular, semi-angular grain/crystal shape. It is also in the form of prismatic crystals with smooth fresh surfaces that do not present twinning. It has light gray-beige birefringence color with orthoclase, semi-shaped, semi-cornered, perthitic (film perthite) structures/exsolutions. In the form of inclusions, the epidote and rutile were observed at a secondary rate. It offers a very mild sericitization and local carbisbad twinning. Plagioclase is oligoclase in the semi-self-shaped, polysynthetic twined, albite section with damping angles of 10–12°. Microcline is semi-self-shaped, semi-cornered, bidirectional polysynthetic twined, and has shades of dark gray-smoked birefringence. Biotite is in the form of semi-intrinsic crystals, mostly chloridized and opaque throughout its cleavages. After chloridization, it has gained light green (grass green) and light brown-yellowish color tones in its birefringence colors. Opaque mineral offers semi-angular, magmatic

eroded, gnawed, gulf structures and local skeletal structures. They are usually distributed in the form of scatters in the tissue. Visually it was defined as magnetite. Aegirine-augite (clino pyroxene) offers self-amorphous, fragmented-fractured, pseudomorphic relic color, high-relief particles distributions.

In the first stage, the grindability value of nepheline syenite is determined. The Hardgrove method (HGI) was used for this. In the coal industry, $13+6.93D_{74}$ (D_{74} represents 74 μm of sieve amount, g). Nepheline syenite was pulverized according to the procedure described in the ASTM D-409-02 standard test method [15] for grindability of coal by ball-race Hardgrove-machine. Then an approximate Bond work index of nepheline syenite was calculated from $W_i = 511/\mathrm{HGI}^{0.96}$ [16, 17]. The calculated HGI is 56.66, W_i—10.60 kW·h/t. In the next stage of nepheline syenite, three different mono-size intervals (–0.090+0.053 mm) were prepared according to the $\sqrt[4]{2}$ sieve series. The specific rate of breakage (S_i) of the classified material for alloy steel balls of diameter 6.35, 7.94, 9.52, 12.70 and 19.05 mm were determined from the formula:

$$S_i = \alpha\left(\frac{x_i}{1\ \mathrm{mm}}\right)^{\alpha} Q_i,$$

where x_i is the upper dimension (mm) of the range i; $\alpha = 0.5-1.5$ is a positive number, normally in the range 0.5 to 1.5, which is characteristic of the material (providing the test conditions are in the normal operating range) but the value of a will vary with mill conditions [13]; $Q_i = 1/[1+(x_i/\mu)]^{\lambda}$ are the correction factors (μ is the size at which $Q_i = 0.5$, $\lambda \geq 0$ is an index of how rapidly the rates of breakage fall as size increases) [13].

In the determination of breakage distribution function for five different ball sizes of nepheline syenite prepared in mono-size intervals, BII method which was developed based on kinetic model was used [13]. The samples prepared for this were milled for the shortest grinding time within a period of time that was used for the grinding of approximately 20–30% of the initial size. At the end of this grinding period, all products were screened and breakage distributions of each raw material were determined from [13]:

$$B_{i,1} \simeq \frac{\log[(1-P_i(0))/(1-P_i(t))]}{\log[(1-P_2(0))/(1-P_2(t))]}, \quad i>1,$$

where $P_i(0)$, $P_2(0)$ cumulative sub-sieve % of the material fed in size range i, %; $P_i(t)$ is the cumulative sub-screen of the material at the time t in the dimension range i. If the top size is denoted by j, the equation above can also be put as:

$$B_{i,j} \simeq \frac{\log[(1-P_i(0))/(1-P_i(t))]}{\log[(1-P_{j+1}(0))/(1-P_{j+1}(t))]}, \quad i>j.$$

Using the nonlinear regression technique, by rendering the sum of the squares of the differences between the measured and calculated values minimal, γ, φ and β parameters were determined. The changes in the breakage distribution parameters and particle size were investigated. It is recalculated from:

$$B_{i,j} = \varphi_j\left(\frac{x_{i-1}}{x_j}\right)^{\gamma} + (1-\varphi_j)\left(\frac{x_{i-1}}{x_j}\right)^{\beta}, \quad 0 \leq \varphi_j \leq 1.$$

In the experiments, 75% of the rotational speed of the ball mill, the critical speed of the mill, N_c, is taken. The ball mill characteristics and test conditions that are used are given below:

Diameter/length of mill, mm	150/150
Volume of mill, m^3	$2.65 \cdot 10^{-3}$
Critical rotational speed of mill, rpm	111–117
Operational rotational speed of mill, rpm	83–88
Ball material	Alloyed steel
Ball diameter, mm	6.35, 7.94, 9.52, 12.70, 19.05
Specific gravity, kg/m^3	8.09
Fractional ball filling	0.30
Specific gravity of milled material, kg/m^3	2.44
Fractional powder filling	0.12
Powder–ball loading ratio	1.00

2. RESULTS AND DISCUSSION

The materials in the mono-size intervals were milled linearly with increasing grinding times. At the end of each milling period, the fractions of material remaining in the top grain size range were plotted against milling times. The results are shown in Fig. 2. The region where the graph decreases linearly represents the first-order breakage region. The slope of the line in the first-order breakage region gives the specific rate of breakage depending on the particle size range of the material.

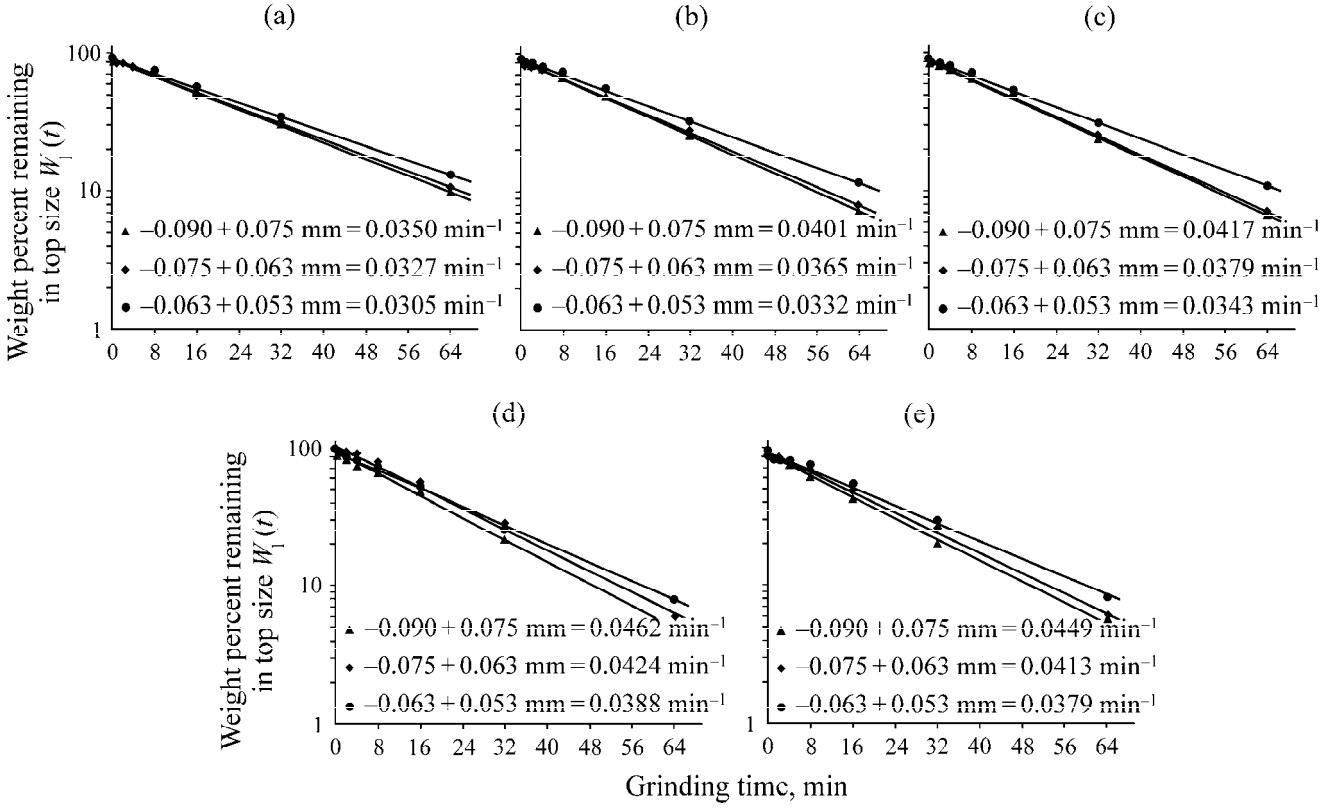

Fig. 2. Rate of breakage with balls of different diameters: (a) 6.35, (b) 7.94, (c) 9.52, (d) 12.70, (e) 19.05 mm.

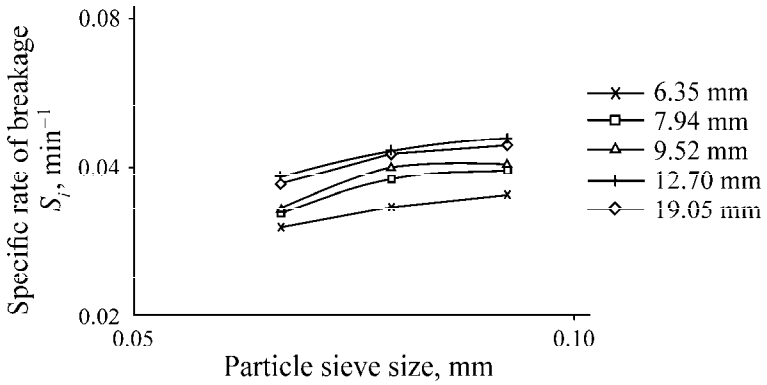

Fig. 3. Variation of specific rate of breakage with ball diameter in dry grinding of nepheline syenite (D=0.15 m, J=0.30, U=1).

Specific rates of breakage, for different sized balls S_i for different sized balls, min^{-1}, are given below:

Feed size, mm	6.35 mm	7.94 mm	9.52 mm	12.70 mm	19.05 mm
0.090–0.075	0.0350	0.0401	0.0417	0.0462	0.0449
0.075–0.063	0.0327	0.0365	0.0379	0.0424	0.0413
0.063–0.053	0.0305	0.0332	0.0343	0.0388	0.0379

After determining the specific rate of breakage for the three mono feed size intervals fractions exhibiting first-order breakage kinetics behavior S_i were plotted against particle size fraction. The rate of breakage parameters of these lines were determined a, α, μ and Λ (Fig. 3).

It is understood from Fig. 3 that specific rates of breakage started to decrease after a grain size of 0.090 mm. The presence of a maximum is quite logical because large lumps obviously will be too strong to be broken in the mill. Austin, Klimpel, and Luckie (1984, 81) consider, "[t]he theory of fracture implies that smaller particles are relatively stronger because larger Griffith flaws exist in larger particles and they are broken out as size is reduced. The fact that the specific rates of breakage are a simple power function of size has not been adequately explained on a theoretical basis, but it has been amply demonstrated by many experiments. The particle size and variations of the breakage distribution parameters were examined and it was found that the data were normalized meaning that they are independent of size. The variation of breakage distributions by particle size is given in Fig. 4.

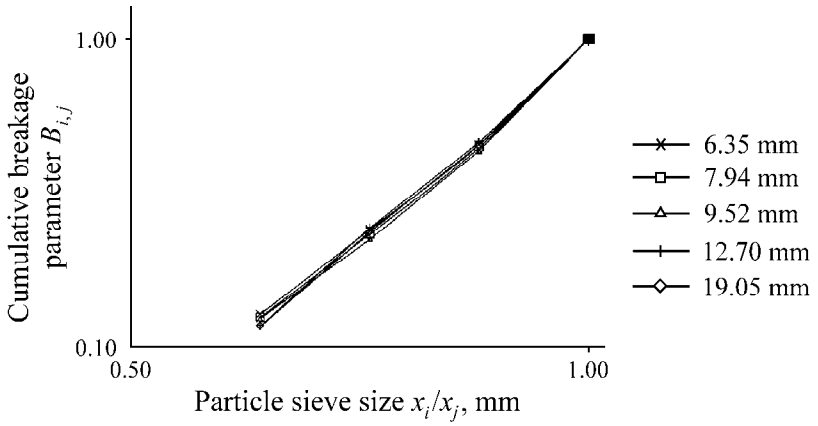

Fig. 4. Cumulative breakage distribution functions for different ball diameter.

Table 1. Model parameter values for different sized balls

d, mm	a, min^{-1}	α	μ	λ	γ	φ_j	β
6.35	0.16	0.57	0.30	1.35	3.830	0.853	11.551
7.94	0.23	0.67	0.39	1.37	3.842	0.835	12.166
9.52	0.24	0.68	0.39	1.37	3.791	0.801	13.026
12.70	0.24	0.63	0.37	1.37	4.152	0.932	7.819
19.05	0.23	0.62	0.36	1.36	4.105	0.902	9.896

Austin, Klimpel, and Luckie (1984) researched the effect of eight balls in the 19–64 mm range in the determination of B parameters of quartz sample. In the study, it was seen that large balls create a greater impact force. It was observed that as the ball size increases, γ value increases meaning that the amount of fine material decreases and φ value increases. According to Austin, Klimpel, and Luckie (1984, 94), "[t]hus, the lower specific rate of breakage due to larger balls is partially compensated by the production of a bigger proportion of fine fragments". In Table 1, it is seen that the opposite occurs for the γ values.

In conventional ball mills, large balls are known to be responsible for the breakage of coarse particles and small balls are supposed to grind the fine ones. Austin, Klimpel, and Luckie (1984, 93–94), stated the effect of ball diameter on rate of breakage as "considering a representative unit volume of mill, the rate of ball-on-ball contacts per unit time will increase as ball diameter decreases because the number of balls in the mill increases as $1/d^3$. Thus the rates of breakage of smaller sizes are higher for smaller ball diameters." However, in the study in question, the specific rate of breakage of the raw material of 0.595–0.420 mm size was determined by using balls in the range of 20–50 mm. The conditions of this study are different. The maximum size of the balls was taken as 19 mm and according to the $\sqrt[4]{2}$ sieve series, three mono-size intervals (–0.090+0.053 mm) were used. Griffith type cracks were reduced and grinding became more difficult as the particle size decreased. In Fig. 5, the specific rate of breakage has also started to decrease as the grinding energy transferred by the small-sized balls onto the particles became insufficient. It is seen that a more effective breakage occurs with large balls. This study was shown that d= 12.70 mm was the optimum ball size for the maximum breakage rates.

In Fig. 6, parameters γ and φ of nepheline syenite in the normal breakage region are observed to vary with the ball size. Finer material was obtained with smaller ball diameters. However, even if the tendency seems to be quite real, the measurement of B values is not clear enough to accurately develop quantitative relationships.

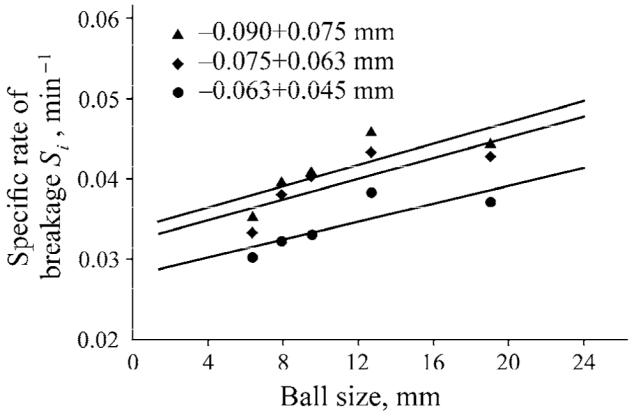

Fig. 5. Variation of specific rate of breakage versus ball diameter in grinding of different particle sizes.

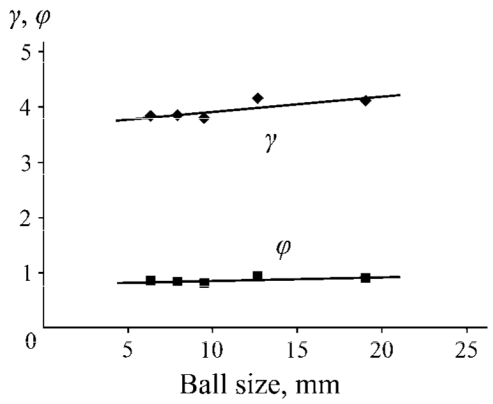

Fig. 6. Variation in γ and φ with ball diameter in dry grinding of nepheline syenite (D= 0.15 m, J= 0.30, U= 1).

CONCLUSIONS

The Hardgrove Grindability Index (HGI) has been determined (HGI = 56.66), and the value of W_i has been calculated on this basis (10.60 kW·h/t). The effect of ball size on the grinding kinetics of nepheline syenite in the ball mill was investigated. According to the dry grinding results of nepheline syenite, the ball diameter followed the first-order breakage law with constant normalized primary breakage distributions. The particle size and variations of the breakage distribution parameters were examined and it was found that the data were normalized meaning that they are independent of size.

In this study, it was found that very small ball sizes could not play an effective role in crushing the material and that their impact on the particles was low. Since the abrasion mechanism is more effective than collision in materials with fine particle sizes, more fine materials that provide a surface area were obtained in small ball sizes. However, since the energy transferred for grinding by the small balls is not sufficient, it provided a more effective breakage by the large balls. In this study carried out with different ball sizes, it was found that the most effective breakage was achieved with $d = 12.70$ mm ball.

As a result, when the literature is examined, breakage data of some raw materials used in various branches of industry cannot be found. Besides, the breakage parameters of the raw material belonging to any region vary according to the mineral content that it contains. Therefore, in ore preparation plants, it is useful to measure the grinding kinetics of raw materials in order to reduce the amount of energy spent for grinding.

FUNDING

The study was supported by the TUBITAK, project name: TUBITAK-MAG-118M224. The author expresses his gratitude to TUBITAK in this regard.

REFERENCES

1. Haner, S. and Demir, M., Nepheline Syenite: A Review, *J. Geol. Eng.*, 2018, vol. 42, no. 1, pp. 107–120.
2. *Feldspar Report*, TMMOB Maden Mühendisleri Odası, Accessed December 15, 2019. www.maden.org.tr/resimler/ekler/8c09c2ec26db837_ek.pdf.
3. Revnivtsev, V.I., Kropanev, S.I., and Peskov, V.V., Methods of Increasing the K_2O:Na_2O Ratio in Feldspars, *Glass and Ceramics*, 1964, vol. 21, no. 1, pp. 32–36.
4. Liddell, K.S., Machines for Fine Milling to Improve the Recovery of Gold from Calcines and Pyrite, *Proc. Int. Conf. on Gold*, Johannesburg, 1986, pp. 405–417.
5. Agrafiotis, C. and Tsoutsos, T., Energy Saving Technologies in the European Ceramic Sector: A Systematic Review, *Appl. Therm. Eng.*, 2001, vol. 21, pp. 1231–1249.
6. Durgut ,E., Pala, Ç.Y., Kayacı, K., Altıntaş, A., Yıldırım, Y., and Ergin, H., Development of a Semi-Wet Process for Ceramic Wall Tile Granule Production, *J. Ceram. Proc. Res.*, 2015, vol. 16, pp. 596–600.
7. Plaksin, I.N., Uteush, E.V., and Uteush, Z.V., Some Problems in Process Control in Enrichment Plants, *Soviet Min. Sci.*, 1965, vol. 1, no. 4, pp. 405–408.
8. Bakker, J., Energy Use of Fine Grinding in Mineral Processing, *Metall. Trans. E*, 2014, vol. 1E, pp. 8–19.
9. Coghill, W.H. and Devaney, F.D., *Ball Mill Grinding*, 1937. Accessed December 15, 2019. play.google.com/books/reader?id=k4MbYBy8674C&hl=tr&pg=GBS.PP1.
10. Bond, F.C., Grinding Ball Size Selection, Min. Eng., 1958, pp. 592–595.

11. Austin, L.G., Shoji, K., and Luckie, P.T., The Effect of Ball Size on Mill Performance, *Powder Technol.*, 1976, vol. 14, pp. 71–79.
12. Yusupov, T.S., Kirillova, E.A., and Denisov, G.A., Dressing of Quartz-Feldspar Ores on the Basis of Selective Grinding and Mechanical Activation, *J. Min. Sci.*, 2003, vol. 39, no. 2, pp. 174–177.
13. Austin, L.G., Klimpel, R.R., and Luckie, P.T., *Process Engineering of Size Reduction: Ball Milling*, New Jersey, American Institute of Min. Metal. and Petrol. Eng. Inc., 1984.
14. Austin, L.G., Bagga, R., and Çelik, M., Breakage Properties of Some Materials in a Laboratory Ball Mill, *Powder Technol.*, 1981, vol. 28, pp. 235–241.
15. *Standard Test Method for Grindability of Coal by Ball-Race Hardgrove-Machine*, Philadelphia, ASTM Int., 1993.
16. Aplan, F.F., The Hardgrove Test for Determining the Grindability Of Coal, *Lecture Note in MN PR 301, Elements of Miner. Proc.*, Pennsylvania State University, State College, Pennsylvania, 1996.
17. Aplan, F.F., Austin, L.G., Bonner, C.M., and Bhatia, V.K., *A Study of Grindability Tests*, G0111786, U. S., Bureau of Mines, U.S.A, 1974.